Multifunctional Structure-Power for Electric Unmanned Systems

J.P. Thomas[*#], **M.A. Qidwai**[†], **J.N. Baucom**[*], **W.R. Pogue**[*]
[*] Multifunctional Materials Branch, Code 6350
US Naval Research Laboratory (NRL)
4555 Overlook Avenue SW
Washington, DC 20375 USA
[#] james.p.thomas@nrl.navy.mil

[†] Science Applications International Corporation (SAIC)
US Naval Research Laboratory Operations
1220 12th St. SE, Suite 140
Washington, DC 20003 USA

ABSTRACT

We provide an overview of recent US Naval Research Laboratory research and development on multifunctional structure-power materials/components for enhancing the performance of unmanned systems through reduction of parasitic (unifunctional) structure mass/volume. Design rules & tools for composite multifunctional materials and three multifunctional structure-power concepts: structure-battery, autophagous (self-consuming) structure-fuel, and solar-skin will be examined. The potential benefits and the technical challenges associated with multifunctional structure-power will be highlighted along with current technological thrusts and possible breakthroughs that can significantly advance the state-of-art.

1.0 INTRODUCTION

Multifunctional materials systems are capable of performing multiple "primary" functions simultaneously or sequentially in time and are specifically developed to improve system performance through consolidation of subsystem materials and functions [1]. The feasibility of a multifunctional material design depends on the internal and external interfacing capabilities and physical/chemical compatibility of the materials required to achieve the desired combination of sub-system functions. The question of which materials and functions to join in a multifunctional material system is best answered by considering the targeted system performance metric expressed in terms of various sub-system design parameters. The combination of structure and battery for use in electric-propelled unmanned air vehicles (UAVs) is a good example of how sub-system materials/functions can be identified for possible integration in a multifunctional material system. For electric-propelled UAVs, an important system performance metric is flight endurance time, which is explicitly related to the available battery energy, subsystem weights, and aerodynamic parameters [2,3]:

$$t_E = \left(\frac{E_B \eta_B}{\left(W_S + W_B + W_{PR} + W_{PL}\right)^{3/2}} \right) \times \left[\frac{\rho S C_L^3}{2 C_D^2} \right]^{1/2} \eta_{M-P}. \quad (1)$$

In Equation (1), E_B is the nominal stored battery energy, η_B is an efficiency factor that accounts for the influence of the current draw rate, temperature, etc., on the amount of energy that can be extracted from the

Thomas, J.P.; Qidwai, M.A.; Baucom, J.N.; Pogue, W.R. (2006) Multifunctional Structure-Power for Electric Unmanned Systems. In *Multifunctional Structures / Integration of Sensors and Antennas* (pp. 1-1 – 1-16). Meeting Proceedings RTO-MP-AVT-141, Paper 1. Neuilly-sur-Seine, France: RTO. Available from: http://www.rto.nato.int/abstracts.asp.

battery. Aircraft structure, battery, propulsion, and payload subsystem weights are represented by: W_S, W_B, W_{PR}, and W_{PL}, respectively. Aerodynamic parameters include: air density, ρ, wing platform area, S, and the lift and drag coefficients, C_L and C_D. Finally, η_{M-P} is the motor/propeller efficiency, which equals the thrust available from the motor/propeller combination divided by the electrical input power to the motor.

Equation (1) shows that combining battery with one of the other sub-systems can provide an increase in flight time by increasing the available energy and/or decreasing the vehicle weight. Empirical data on the weight fractions of various aircraft sub-systems show that structure and fuel (battery) each contribute 20-40% to the total weight of the aircraft (UAV) [3]. This supports the notion of achieving increases in UAV flight time through combining structure with battery in a multifunctional material. The use of multifunctional structure-battery in a UAV influences the flight endurance time through changes in available energy and the structure and battery weights. The normalized change in flight time endurance [3]:

$$\frac{\Delta t_E}{t_E} = \frac{\Delta\left(E_B \eta_B\right)}{E_B \eta_B} - \frac{3}{2}\frac{\left(\Delta W_S + \Delta W_B\right)}{W_{total}}. \tag{2}$$

shows that decreases in vehicle weight are one-and-a-half times more effective in increasing endurance than increases in the stored battery energy capacity.

The constituents in multifunctional materials are often disparate in nature with widely differing property values. This has led to the need for new analysis tools and design methodologies for relating constituent properties and cross-section architecture to system-level performance. Our experiences in developing structure-battery materials have led us to several "Rules" that can help in guiding the material designer achieve maximal gains in system performance through multifunctionality [4]:

- Add new functionality to the material with the more complex base function.
- Target unifunctional subsystem materials/components operating in the mid-to-lower functional performance regimes for replacement by multifunctional materials/components
- Implement multifunctionality in the conceptual stage of system design

The "Materials Selection" approach, developed by Ashby et al. [5] is a useful method for ranking the performance of materials and cross-section shape with respect to system-related objectives like mass, volume, or cost. Modifications are needed, however, for non-homogeneous composite materials because of the interrelated way that the material and the cross-section geometry variables mix in the basic mechanics expressions for stresses and deflections [6]. We have developed a new methodology for deriving performance indices that can be used to rank composite material design configurations relative to an arbitrary user defined objective (e.g., minimize mass) under a variety of loading and deflection constraint conditions [6]. These new performance metrics for composite materials are denoted as material-architecture indices, $\mathcal{MA}$. The methodology is an extension of the Ashby methods wherein modulus-weighted cross-section parameters are employed in the mechanical analysis allowing for the direct use of standard "Mechanics of Materials" equations.

As an example, consider the selection of constituents and the cross-section arrangement for a composite beam of minimum mass with maximal bending stiffness. The system (beam) mass, *m*, is inversely proportional to the material-architecture index, $\mathcal{MA}$, for a composite beam in bending with an end-deflection constraint [6]:

$$m \propto \frac{1}{\mathcal{MA}}, \qquad \text{where}$$
$$\mathcal{MA} = \frac{\left[E_R \phi_B^{*e}\right]^{1/2}}{\rho} = 2\sqrt{\pi}\,\frac{\left[E_R I_{zz}^{*}\right]^{1/2}}{\sum_i \rho_i A_i} \tag{3}$$

In Equation (3), E_R is an arbitrary reference modulus, ρ_i are the cross-section component's densities, A_i are the cross-section areas, and I_{zz}^* is the modulus-weighted 2nd moment of inertia of area about the bending axis. The composite shape factor, $\phi_B^{*e} := 4\pi I_{zz}^* / A^2$, accounts for the effect of the cross-section component modulus values, geometries and arrangements on the bending performance. The $\mathcal{MA}$ indices are independent from the load-related variables and reduce to the classical Ashby material-shape indices when there is only one material constituent (i.e., $E\phi_B$ for bending in non-circular cross-sections). There are multiple design (free) variables in the expression for $\mathcal{MA}$ that lead to the need for more sophisticated material optimization procedures. The additional degrees of freedom provide an opportunity, however, to achieve superior material performance through arrangement of the cross-section architecture, especially in multifunctional composites where large differences in constituent properties often exist.

Other electric energy storage devices like fuel cells, super/ultracapacitors, or capacitors may also be usefully employed in multifunctional structure-energy roles [7]. Each of these devices has different power-energy capabilities (Figure 1). Some low power systems (<<1 watt), such as remote or embedded sensors, may be difficult to access and may be required to function over an extended period of time (e.g., years). Integrated energy harvesting devices like piezo-vibration generators are being investigated for this purpose. Mid-range power applications (~1-1000 watts), such as electric unmanned air vehicles, have stringent weight restrictions and mission times on the order of hours. High specific energy batteries (lithium-ion cells) are currently serving this need as unifunctional energy sources or in the form of multifunctional structure-battery [4, 11]. There is also significant interest in developing fuel cells for these medium-power applications. High power applications (>1000 watts) generally involve systems and vehicles with large structures that may be amenable to integration with energy storage (e.g., structure-capacitor) and energy scavenging (e.g., solar cells) functionalities.

Multifunctional structure-power components can be developed by adding structural functionality to an existing energy storage material or by adding energy storage functionality to an existing structural material. Adding new functionality to the material with the more complex base function will likely produce the best gains in system performance (Rule #1(. Figure 2 shows the energy storage capacity for a variety of solid, liquid, and gaseous hydrocarbon materials and electrochemical battery systems plotted on a per unit mass (specific energy) versus per unit volume (energy density) basis. The battery data other than LiF includes packaging and auxiliary mass (electrolyte, current collection materials, electrodes, etc.) in the energy values while the hydrocarbon fuels, plastics, and LiF battery data pertain only to the active materials. Packaging/auxiliary mass can account for a large fraction (>50%) of total energy system mass, particularly as the physical size decreases. The autophagous structure-fuel concept developed at NRL [9] utilizes the vapor-pressure of a two-phase (liquid/gas) hydrocarbon fuel to rigidize and strengthen a light-weight composite structural shell. The pressure keeps the lightweight, high-stiffness composite shell layers expanded to their outermost position to maintain maximal bending performance and to prevent failure by local elastic buckling.

The third structure-power concept, solar-skin, utilizes scavenged solar energy to extend the mission endurance and range of electric unmanned systems [10]. Replacement of unifunctional skin-structure with solar panels capable of providing both structure and energy collection functions can supplement the on-board power source at various levels depending on the available surface area for energy collection and the balance between scavenged power levels and solar scavenger weight. An overview of commercial photovoltaic technology will be given, and an analysis methodology will be demonstrated for linking unmanned air vehicle (UAV) performance to the UAV power supply design variables.

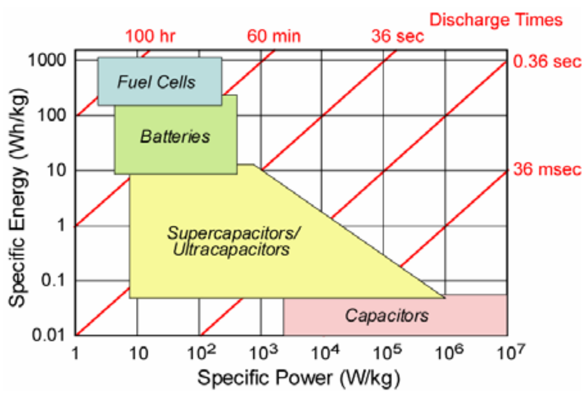

Figure 1: Ragone plot showing energy storage-delivery performance for various energy storage devices (following [8]). The red lines indicate times for complete discharge of the stored energy.

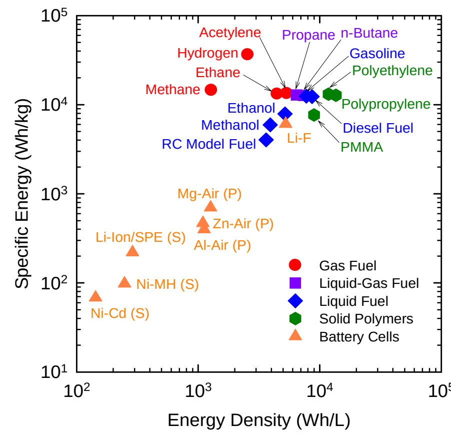

Figure 2: Energy storage performance for hydrocarbon fuels and batteries at room temperature. (P) = primary, (S) = secondary

2.0 MULTIFUNCTIONAL STRUCTURE-POWER SYSTEMS

2.1 Structure-Battery Composites

Adding structure function to an existing battery system may be the best strategy for creating structure-battery materials due to the complexity of the energy storage process relative to that of elastic deformation of a structural material (Rule #1). Figure 2 shows the energy storage capacity for representative primary (one-time-use) and secondary (rechargeable) battery cells normalized by volume and mass. For rechargeable cells, the lithium batteries stand out with their high energy storage capacities. The polymer lithium-ion intercalation cells (Li-Ion (S)) are particularly desirable because of their layered construction, soft packaging, safe-failure modes, and wide-spread commercial availability. The following example considers multifunctional performance of notional structure-battery beams in cantilever bending.

2.1.1 Structure-Battery Design Example

The previously described analysis methodology can be used to obtain mechanical performance indices for the composite structure-battery beam configurations shown in Figure 3. The basic design is a cantilevered beam under pure bending with one or more battery bicell layers that are stacked and packed with or without mechanical reinforcement. The “control” configuration consists of only bicell layers and packaging with no mechanical reinforcement. A second configuration incorporates a woven carbon fiber cloth layer between the packaging and bicell core stack, and the third adds a unidirectional carbon-fiber-epoxy layer to the outside of the packaging. Each reinforcement layer is approximately 0.2 mm thick (one-ply), roughly one-half the thickness of one bicell layer. Additional details can be found in [6].

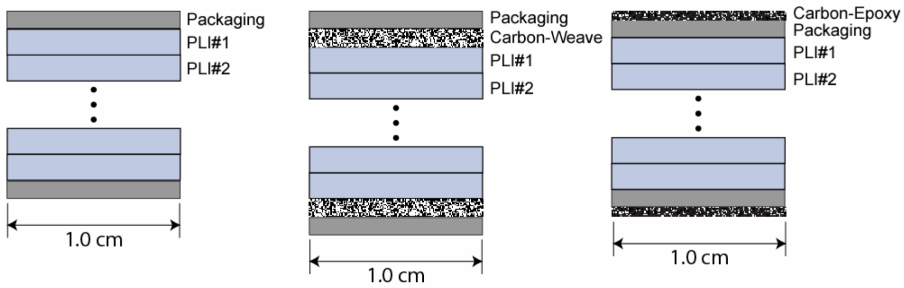

Figure 3: Notional structure-battery configurations. PLI designates plastic-lithium-ion bicell layers.

Multifunctional performance of the structure-battery beams, shown in Figure 4, consists of $\mathcal{MA}$ for bending stiffness versus specific energy. Both $\mathcal{MA}$ and specific energy are inversely proportional to the beam mass per unit length for a given limit on bending deflection and a required energy storage capacity. Best multifunctional performance (lowest mass in this case) corresponds to the upper right-hand corner of the plot. The carbon-epoxy reinforced structure-battery show the best stiffness per unit mass, and the plain packaging shows the best energy capacity per unit mass. Specific energy increases with number of bicell layers in all configurations due to the increasing fraction of energy-storage materials in the laminate. The specific energy approaches that of the bicell alone (~165 Wh/kg in this analysis) as the number of bicell layers increases.

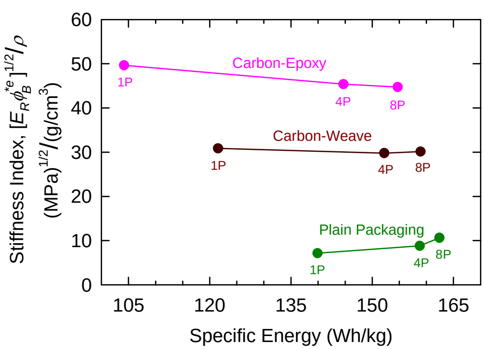

Figure 4: Multifunctional performance for the three notional structure-battery beam designs with one, four, or eight (1P, 4P, or 8P) plastic-lithium-ion bicell layers. Beam mass is minimized in the upper right corner.

Figure 5: First generation DARPA Wasp micro-air vehicle showing custom batteries (silver quadrilaterals, top and bottom) integrated as wing-skin at the leading-outboard-edges.

The selection of a particular configuration will depend on requirements related to bending stiffness, energy storage, and other constraints (e.g., beam thickness). The carbon-fiber-epoxy reinforcement provides the highest mechanical stiffness per unit weight. The plain-packaged beam provides the highest energy storage capacity per unit weight. The carbon-fiber-epoxy configuration provides the best overall multifunctional performance and has the added advantage that the external reinforcement can be added after battery fabrication. The maximum cure temperature during the external reinforcement processing must be kept lower than 80-90$^\circ C$, however, to avoid damaging the cells through electrolyte boiling/outgassing.

2.1.2 Structure-Battery in the Wasp Micro-Air Vehicle

Multifunctional structure-battery is being used in the Wasp micro-air vehicle developed under DARPA sponsorship [11]. The Wasp is a radio-controlled, "flying-wing" aircraft developed for intelligence, surveillance and reconnaissance by AeroVironment, Inc. of Simi Valley, CA. The original prototype, shown in Figure 5, has a ~32 cm wingspan and weighs 171 grams with 98 grams of polymer lithium-ion structure-battery in the wing. It achieved a record-setting endurance time of 1 hour 47 minutes on one charge. The four embedded structure-battery cells were fabricated by Telcordia Technologies of Red Bank, NJ and were combined in a two-parallel-two-series configuration giving 1.8 Ah capacity at ~7.5 V volts with an average power draw rate during steady-level flight of 7.6 W. The specific energy of the cells was 136 Wh/kg.

2.2 Autophagous Structure-Fuel System

Autophagous structure-power refers to "self-consuming" components that are multifunctional in the sense of being able to carrying mechanical loads and provide useful system energy through a physical/chemical transformation process. The structure and power functions may occur simultaneously, with constituents that carry mechanical loads while concurrently providing system power, or sequentially, with constituents that carry mechanical loads for some fixed period of time after which they are transformed and consumed to provide system power. The potential loss of structural capability and the loss of mass as material is consumed for power must be taken into account in the system/component design. Multi-mode missions with large changes in structural requirements during the course of a mission can take advantage of sequential autophagous structure-power. Examples include: space satellites with large launch loads and lower orbit loads, or an expendable unmanned air vehicle designed to transport a sensor(s) to a desired location where it lands and serves thereafter as a non-flying platform for sensor power, communications, etc. Launch or flight related structure (e.g., internal struts, wings, empennage, etc.) may not be needed in later phases of the mission, and this structure can be consumed to provide additional system power.

2.2.1 Autophagous GasSpar

The autophagous GasSpar system uses the vapor pressure of a two-phase liquid-gaseous butane or propane fuel to stiffen and strengthen an inflatable composite beam [9]. The fuel can directly power an internal combustion engine or solid-oxide fuel cell, or it can be combusted and used to create electricity via thermoelectric conversion. A notional GasSpar system for an electric UAV is shown in Figure 6. It consists of a GasSpar in the aircraft wing with a converter in the fuselage to burn the fuel and create electric power using thermoelectric Bi_2Te_3 modules. The GasSpar beam is a lightweight, flexible composite shell with an internal polymer "bladder" for fuel containment. Butane or propane pressurizes the bladder expanding and maintaining the cross-section to maximize bending stiffness and strength. The pressurized fuel serves as the structural core material (typically polymer foam or honeycomb) and the bladder as the gas storage tank. The pressure of a saturated gas in equilibrium with its liquid phase depends on temperature alone (see Figure 7), and this pressure remains constant (assuming constant temperature) as long as any liquid phase remains. The constant pressure of the equilibrium liquid-gas mixture provides GasSpar with a constant level of mechanical performance until all of the fuel is consumed.

Butane and propane fuels for GasSpar are readily available, have high heats of combustion (~12,800 Wh/kg), a wide range of pressures, and burn cleanly. They can be mixed to tailor the pressure-temperature curve and achieve the desired mechanical performance over a range of operational temperatures. The power per unit mass of the GasSpar system equals the electrical output power of the thermoelectric generator(s) divided by the total system mass. Specific energy of the GasSpar system is determined by the amount of fuel stored in

GasSpar, the efficiency of the combustion and conversion processes, and the total system mass. For the GasSpar autophagous energy system to achieve a specific energy of 200 Wh kg^{-1} and match that of state-of-the-art commercial Li-ion secondary cells, the following conditions must be met:

$$\frac{\text{Fuel Mass}}{\text{System Mass}} \times \frac{\text{Thermoelectric Input Energy}}{\text{Theoretical Combustion Energy}} = \eta_{mass} \times \eta_{combustion-transfer} > 37\% \quad (4)$$

The 37% value on the right-hand side is obtained by dividing target performance, 200 Wh/kg, by the specific energy of n-butane (12,800 Wh/kg), then dividing by 5%, an assumed heat-to-electricity conversion efficiency for the thermoelectric module(s), and then dividing by 85%, an assumed efficiency for DC power conditioning. On the left hand side, the first term accounts for the proportion of system mass taken up by the energy producing n-butane fuel. The second term accounts for the proportion of theoretical fuel energy that is actually transported through the thermoelectric module(s) for conversion to electricity. The 37% value can be achieved if the individual mass and combustion-transfer factors are each greater than 60%. Increasing the fuel storage volume and/or decreasing the combustion-converter weight will increase the fuel mass fraction, and thermal design optimization can be used to increase the combustion efficiency.

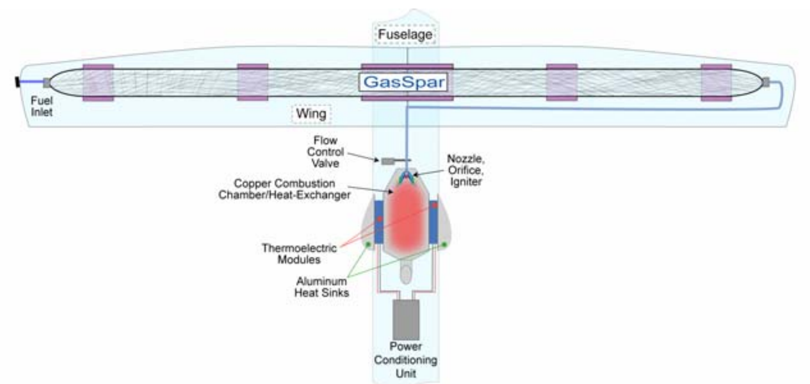

Figure 6: Notional autophagous structure-power system for an unmanned air vehicle. GasSpar forms the main structural element of the aircraft wing, and a combustion thermoelectric conversion process is used to convert the two-phase hydrocarbon fuel stored inside GasSpar into electricity.

A first-generation GasSpar system prototype developed at the Naval Research Laboratory [9] demonstrated a 20 Wh/kg specific energy at 2.9 W/kg specific power with approximately 7 hours of burn time for a total of 8.4 Wh usable electrical energy. The GasSpar beam itself is 1.9 cm in diameter, 46 cm in length, and weighs 46 g empty (Figure 8). The fuel bladder was constructed of a chemically compatible polymer (C-Lam) with polyethylene end plugs by ATL, Inc. The bladder was wrapped with Kevlar cloth (two layers) to prevent outward blistering when under pressure. Four thin (0.13 mm) unidirectionally reinforced carbon epoxy strips were positioned around the circumference of the tube as load-bearing spar caps. The strips have a high modulus in tension and compression; however, their small thickness makes them prone to buckling in compression. The internal fuel pressure prevents inward buckling of the strips when the spar is loading in bending and results in a beam with high second moment of inertia. Woven carbon/epoxy end caps were fabricated to join the ends of the lateral strips. To prevent outward buckling of the strips, the spar was wrapped at intervals along the length with Kevlar thread which was then sealed with a small amount of epoxy. The spacing, which varies linearly along the length with smaller spacing at the root end, was determined by consideration of expected loads and Euler buckling theory. Total system mass is 420g with 303g of thermoelectric combustion-converter and 70g of n-butane fuel (880 Wh of chemical energy). The core volume of GasSpar is ~ 130 cm^2, which would be filled with ~7-40 g of polymer foam, depending on the structural design requirements. The overall conversion efficiency of this proof-of-concept prototype is ~1%. The n-butane fuel provides 117 kPa of vapor pressure at room temperature resulting in a measured 2.5-fold increase in bending stiffness and 4.2-fold increase in bend-buckling strength over the unfilled beam.

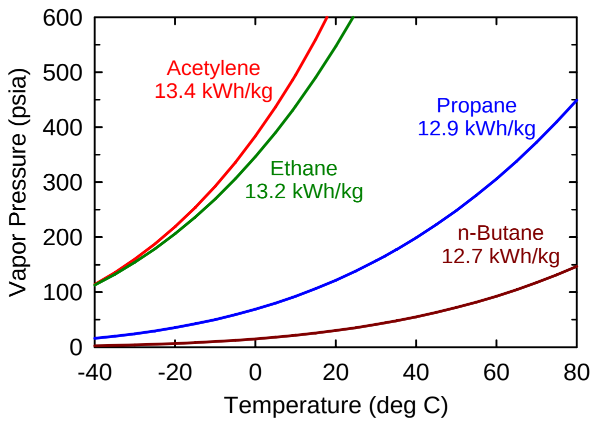

Figure 7: Vapor pressure-temperature plots for acetylene, ethane, propane, and n-butane. At 20°C, their vapor pressures are: 610, 520, 125, and 30 psia, respectively. Data from: http://webbook.nist.gov/chemistry/fluid/.

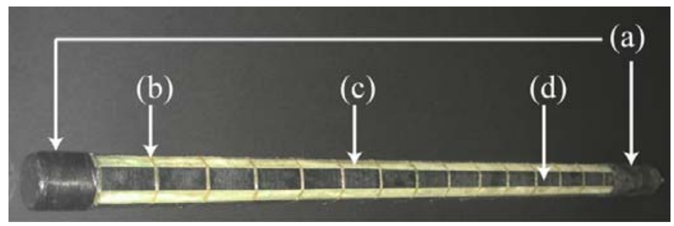

Figure 8: GasSpar: (a) carbon/epoxy end-caps, (b) Kevlar thread hoop-wrap, (c) woven Kevlar thread, (d) unidirectionally reinforced carbon/epoxy strips.

Significant improvements in the overall system efficiency and specific energy and power values can be achieved through design improvements in the hot and cold-side heat exchangers and burner, and reductions in component weights, especially those associated with the combustion-converter. Key implementation issues for GasSpar structure-power systems include the design and fabrication of multifunctional structural components that optimally utilize the fuel vapor pressure to achieve mechanical performance and the need for efficient, lightweight chemical-to-electric conversion devices.

2.3 Solar-Skin

A wide variety of large and small unmanned systems are being developed and used by government and industry for sensing and other missions on land, in the air, in or on the water, and in space. The system's size, weight, and operational requirements related to mobility, range, and time-on-station dictate the power needed, and the on-board energy storage capacity is governed by the volume and weight available for the energy storage device(s). Supplementing the on-board energy stores with energy scavenged in-the-field can provide a new capability for extending the endurance and range of electric-powered unmanned systems.

2.3.1 Solar Energy Harvesting

Photonic energy (photon radiation) is readily available outdoors and in artificially lighted indoor locations. Approximately 1000 W/m^2 of solar power is incident on surfaces directly facing the sun on a bright sunny day [12]. Photonic energy can be converted directly to electricity using photovoltaic (solar) cells made from semiconductor materials. Solar cell arrays or panels may also be integrated as multifunctional structural skin in order to provide some mechanical function, which may allow for a reduction in structural mass.

Characteristic current versus voltage (*I-V*) performance for p-n type solar cells is shown in Figure 9. The short-circuit current, I_{sc}, and the open circuit voltage, V_{oc}, are two defining characteristics of a solar cell. Together with maximum cell output power, P_{max}, they are used to define the fill factor, *FF* [13]:

$$FF := \frac{P_{\max}}{I_{sc} \times V_{oc}} \quad (5)$$

The fill factor is a measure of cell quality ranging from 0 (poor) to 100% (excellent). A typical (large-scale) solar power generation system consists of a solar cell array (collector), blocking diodes, a peak power controller to maintain the output current and voltage at maximum power output level (i.e., the knee of the I-V curve), and optional sun tracking controls (Figure 10). Blocking diodes and fuses are incorporated to prevent discharge of the battery when the solar panel is not illuminated and to protect against large currents that can develop under ground-faulting conditions. Sun tracking controls ensure that the solar array is oriented perpendicular to the sun's rays to maximize the direct radiation exposure from the sun.

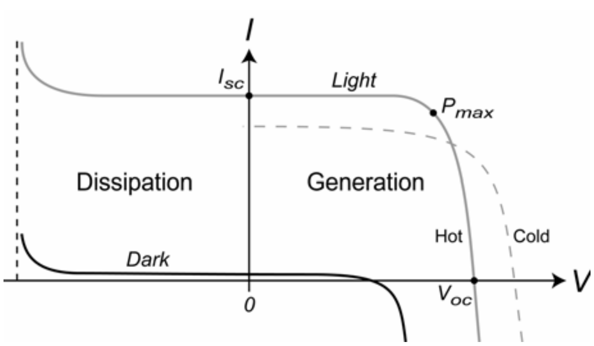

Figure 9: Current-voltage behavior of silicon photovoltaic cells with (light) and without (dark) incident radiation. Decreasing cell temperature lowers the short-circuit current, I_{sc}, and increases the open-circuit voltage, V_{oc}, leading to a net increase in output power.

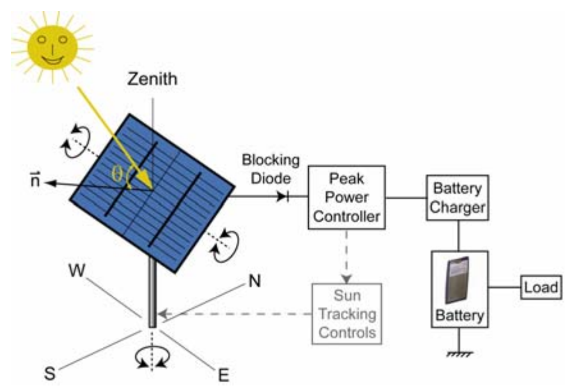

Figure 10: Typical solar generation system. Major components include the: solar collectors, blocking diode, peak power controller and (optional) sun tracking controls.

The efficiency of conversion from photonic to electrical energy is practically constant over a wide range of incident radiation. Commercial solar conversion efficiencies range from a low of approximately 8% to state-of-art values of 30% or more [14]; some experimental technologies reach as high as 35%. The most common material used in photovoltaic cells is crystalline silicon (c-Si) in single crystal, polycrystal, ribbon and sheet, and thin-layer forms. Efficiencies range from 10% to 23% in state-of-the-art cells. Other solar technologies include the high efficiency multi-junction devices, which stack different photovoltaic cells on top of each other to maximize the capture of incident radiation, and thin film flexible solar cells. Solar panel sizing, power control, and multifunctional integration are key implementation issues for photonic energy scavenging.

2.3.2 Solar Scavenger Design Study

The following example illustrates a method for linking unmanned air vehicle (UAV) performance to power supply (battery and solar scavenger) design variables [10]. Assume that the flight endurance time (t_E) of an electric UAV under steady-level flight conditions is the primary system performance metric. An equation for t_E with both battery and solar scavenging power sources can be obtained by modifying Equation (1):

$$t_E = \left(\frac{E_B \eta_B + P_{SC} t_E}{W_T^{3/2}} \right) \times \left[\frac{\rho S C_L^3}{2 C_D^2} \right]^{1/2} \eta_{M\text{-}P} \rightarrow t_E = \frac{E_B \eta_B}{\left(W_T^{3/2} - P_{SC} \left[\frac{\rho S C_L^3}{2 C_D^2} \right]^{1/2} \eta_{M\text{-}P} \right)} \times \left[\frac{\rho S C_L^3}{2 C_D^2} \right]^{1/2} \eta_{M\text{-}P} \tag{6}$$

where W_T is the total vehicle weight ($m_T g$) and P_{SC} is the solar scavenger output power. Normalized change in endurance, $\Delta t_E / t_E$, as a function of changes in battery energy, subsystem weights, and/or scavenger power can be approximated using a Taylor series expansion of Δt_E about the point $P_{SC} = 0$ (i.e., linear extrapolation from the non-solar design):

$$\frac{\Delta t_E}{t_E} = \frac{\Delta E_B}{E_B} - \frac{3}{2} \frac{\Delta W_T}{W_T} + \frac{\Delta P_{SC}}{E_B / t_E} = \frac{\Delta m_B}{m_B} - \frac{3}{2} \frac{\Delta m_B + \Delta m_{ST} + \Delta m_{SC}}{m_T} + \frac{p_{SC}}{p_{ave}} \frac{\Delta m_{SC}}{m_B} \tag{7}$$

Δm_B , Δm_{ST} , Δm_{SC} denote the changes in battery, structure, and photonic scavenger masses, p_{SC} denotes the specific power of the solar scavenger system (output power per unit scavenger system mass), and $p_{ave} = E_B \eta_B / m_B t_E$ is the average specific power supplied by the battery in the non-solar version of the UAV. Equation (7) can be used to assess the influence of solar scavenging on the UAVs flight endurance time.

For example, consider the following five design scenarios: **1.)** add a solar scavenger system to the UAV without changing the existing battery or vehicle structure weights; **2.)** add a solar scavenger system to the UAV and remove an equal amount of battery weight while keeping the structure weight constant; **3.)** add a solar scavenger system to the UAV and remove an equal amount of structure weight while keeping the battery weight constant (multifunctional solution); and **4a.)** add more battery to the UAV without adding a solar scavenger and without changing the structure weight, or **4b.)** add more battery to the UAV and remove an equal amount of structure weight, again without adding a scavenger system (multifunctional solution). Cases 4a and 4b serve as “standards” for comparing solar scavenging with battery addition as a means of increasing UAV endurance. Cases 1 and 4a consider changes in endurance through solar scavenger or battery addition, respectively, without any other design changes. Cases 3 and 4b consider changes in endurance through substitution of solar scavenger or battery weight, respectively, for UAV structure (multifunctional design). Case 2 is similar to Case 3 except that solar scavenger weight is substituted for battery weight.

Table 5 summarizes the general relations derived from Equation (7) for each of the design scenarios and their application in each case to a notional micro-UAV with the following specifications: total vehicle mass of 225 grams, 75 g of secondary lithium-ion cells with 200 Wh/kg providing a total of 15 Wh of battery energy, 30 minutes of flight endurance time, and 400 cm^2 wing area. The wing area defines a limit on the maximum number of solar cells (N) that can be attached to the UAV; $N \approx S / A_{SC}$ where S is the wing planform area and A_{SC} is the area per solar cell. The two right columns in Table 5 correspond to micro-UAV calculations.

Table 5: Expressions for the normalized change in flight endurance time.

Case	Conditions	Normalized Change in Flight Endurance, $\Delta t_E / t_E$	$\left(\Delta t_E / t_E\right)_{m-UAV}$	Rank
1	$\Delta m_B = \Delta m_{ST} = 0$	$-\frac{3}{2}\frac{\Delta m_{SC}}{m_T} + \frac{p_{SC}}{p_{ave}}\frac{\Delta m_{SC}}{m_B}$	$\left\{-0.0067 + 3.33\times 10^{-5} p_{SC}\right\}\Delta m_{SC}$	2
2	$\Delta m_B = -\Delta m_{SC}$ $\Delta m_{ST} = 0$	$-\frac{\Delta m_{SC}}{m_B} + \frac{p_{SC}}{p_{ave}}\frac{\Delta m_{SC}}{m_B}$	$\left\{-0.0133 + 3.33\times 10^{-5} p_{SC}\right\}\Delta m_{SC}$	3
3	$\Delta m_{ST} = -\Delta m_{SC}$ $\Delta m_B = 0$	$\frac{p_{SC}}{p_{ave}}\frac{\Delta m_{SC}}{m_B}$	$\left\{3.33\times 10^{-5} p_{SC}\right\}\Delta m_{SC}$	1
4a	$\Delta m_{SC} = \Delta m_{ST} = 0$	$\frac{\Delta m_B}{m_B} - \frac{3}{2}\frac{\Delta m_B}{m_T}$	$\left\{0.0067\right\}\Delta m_B$	2
4b	$\Delta m_{ST} = -\Delta m_B$ $\Delta m_{SC} = 0$	$\frac{\Delta m_B}{m_B}$	$\left\{0.0133\right\}\Delta m_B$	1

Equating the expressions for normalized change in endurance for the micro-UAV between Case 1 and 4a and between Case 3 and 4b, we find that the solar scavenger system must have a specific power value:

$$p_{SC} \geq 400\ \frac{\text{W}}{\text{kg}} \tag{8}$$

in order to increase the micro-UAV endurance beyond that which can be achieved by simply adding more battery. Examination of these expressions also shows that the largest increase in endurance occurs with the multifunctional designs (Cases 3 and 4b) that replace structure with multifunctional structure-scavenger or structure-battery "materials" gram-for-gram. The least effective design appears to be Case 2, which replaces battery with solar scavenger. Adding solar scavenging or more battery to an existing UAV without any other design changes (i.e., Cases 1 and 4a) achieves results that are intermediate to the multifunctional (3,4b) and battery replacement (2) design configurations.

The specific powers for currently available commercial solar cells range from 180 to 560 W/kg for 1000 W/m^2 of incident solar radiation at a zero incidence angle [10]. These specific power refer to the photovoltaic cell itself and do not include the effects of angle of incidence and weight of necessary auxiliary hardware needed by the scavenging system (e.g., solar incident wiring, diodes, power-conditioning electronics, and cell attachment adhesive/framing). An approximate derate factor for short UAV flights at noon in Baltimore (Maryland, USA) would be $F_{SC} \approx 0.6$ (i.e., $\cos(39.19^o)$), and an overall incidence/loss/weight derating factor [10]: $F_{SC} = F_{IAD} \times F_{LOSS} \times F_{WGT} = 0.471$ is used to "uprate" the specific power requirement for the solar cells for the notional micro-UAV:

$$p_{SC} \geq \frac{400}{0.471} = 849\,\frac{\text{W}}{\text{kg}} \tag{9}$$

The analysis shows that solar cells with a specific power greater than 849 W/kg are required to achieve an increase in flight endurance time greater that which can be obtained by simply adding more battery to the aircraft. For the notional micro-UAV of this example, we cannot meet the required solar cell performance with any of the presently available commercial cells. Adding battery is more effective in increasing endurance, in this example, than adding solar scavenging.

If the UAV mission is such that it requires in-the-field recharging that can only be achieved using solar scavenging, then the requirement expressed by Equation (9) must be relaxed. If we drop that requirement that the solar scavenger be more effective than battery and only require that it leads to a positive increase in endurance (i.e., $\Delta t_E \geq 0$), then the expressions in Table 5 show that the flight endurance time increases when $p_{SC} \geq 0$ for Case 3 (multifunction swap of structure for scavenger) or when $p_{SC} \geq 200/0.471 = 425$ W/kg for Case 1 (addition of scavenger). Multifunctional swapping of solar scavenger mass for structure mass will always provide an increase in endurance, regardless of the solar scavenger system efficiency. If the solar scavenger is added to the micro-UAV without any other changes, then solar cells with a specific power greater than 425 W/kg are required to achieve an increase in flight endurance time. The SunPower Pegasus® cells used on AeroVironment's Pathfinder and Helios solar-powered UAVs meet this specific power requirement.

3.0 DISCUSSION AND CONCLUSIONS

Multifunctional design, in the context of this work, seeks reductions in system weight through replacement of parasitic system structure with load-bearing components of the energy storage or scavenging system. The design of structure-power sub-system should be guided by the improvement it affords in the unmanned system's performance (e.g., endurance time, mobile range, communications range, etc.). To assess a particular design, quantitative models are needed that relate the unmanned system's performance to its energy storage and power dissipation (e.g., propulsion, control, sensing, etc.) components and characteristics.

Every unmanned system will have power requirements that are defined by the characteristics of the power dissipating components and the mission particulars. For example, an electric unmanned air vehicle (UAV) may be utilized to provide real-time video imagery of a distant "target." The aircraft's propulsion motor-propeller combination, avionics, video camera, and transmitters all have power requirements that may change with each phase of the mission: launch, climb to altitude, steady-level flight to "target", descent, loiter in surveillance, climb to altitude, steady-level flight back "home", descent, and landing. The total power required during each phase can be determined and integrated over time to determine the total energy required for a mission. Design and optimization of the sub-systems (e.g., power-supply, motor-propeller, aerodynamics, etc.), which are mathematically coupled with the system performance metric, can be performed to minimize the energy/power required during the various phases of the mission.

Improving and optimizing the multifunctional performance of structure-battery materials is a long-range challenge. From a structural point-of-view, the critical issues are: 1.) achieving good load transfer from the structure through the structure-battery packaging to the active energy storage materials inside the packaging, and 2.) possible mechanical reinforcement schemes. Packaging is required for all battery cells, and load transfer through the packaging is a problem. The active electrode materials consist of particles embedded in polymer matrix, which places severe limitations on the mechanical performance. The best mechanical performance can be achieved by volumetrically constraining the active material layers. Incorporating mechanical reinforcement layers in the structure-battery with through-the-thickness “riveting”, similar to the Philips Lithylene® technology, is a promising approach to enhance the mechanical performance of structure-battery components.

From an electrical point-of-view, we want to move the technology towards higher specific energies with corresponding increases in specific power. Research is active on hybrid energy storage technologies that combine battery and supercapacitor electrodes to achieve improvements in performance. Research on three-dimensional lithium-ion cells with networked electrodes and improved power delivery is also ongoing.

Many substances have high specific energies and volumetric energy densities (recall Figure 2). Features of an ideal fuel include high combustion-heat per unit mass (specific energy), as well as per unit volume (volumetric energy density). In selection of a fuel, these parameters must be considered with respect to system requirements. For example, liquid hydrogen has an extraordinarily high specific energy but relatively low energy density. For the purpose of lifting spacecraft into orbit where vehicle mass is a prime consideration, hydrogen is an appealing fuel. Other fuels, like polypropylene, have lower specific energy but higher energy density. In combination with desirable mechanical properties such as stiffness and strength, polypropylene may be preferred for certain multifunctional applications. Hydrocarbon fuels can be used with a solid oxide fuel cell to provide electricity, or they can be combusted to provide large amounts of heat energy. The heat energy must be transformed into electricity using a heat-to-electricity conversion process, but the thermoelectric conversion process is relatively inefficient with a significant fraction of system mass taken up by auxiliary components.

The solar scavenger design study showed how quantitative system performance metrics, flight endurance time in this case, can be used to assess design options related to the energy scavenging and storage subsystems. Additional system requirements/constraints not addressed by the primary system performance metric are often necessary and will influence the design solution space. The requirement for in-the-field solar charging capability is an example; it opened-up the design space so that “sub-optimal” solar cells (425 W/kg versus 850 W/kg) became viable options. Refinements of the analysis are also possible by going beyond the Taylor series expansion (linear extrapolation) for Δt_E, using actual solar radiation data for the operational locations and mission times, and by considering combinations of the three design scenarios. Weight savings through structural function of the solar cells was not discussed, but can also have an impact on system performance.

In conclusion, we selected an example application (electric unmanned air vehicles) with a quantifiable system metric (flight endurance time) to demonstrate the potential of multifunctional structure-power. The analyses and methodologies introduced can be coupled with advanced multi-disciplinary design software and databases to develop and refine multifunctional designs. However, there is a need for more “free-ranging” design assessment procedures for judging multifunctional efficacy. That is, we would like to compare system performance between the optimal multifunctional design and the optimal unifunctional design. Each of these designs may be very different in their details. Obtaining such estimates/data without developing, building, and testing two separate system designs is the challenge.

ACKNOWLEDGEMENTS

Support by the Defence Advanced Research Projects Agency under the Synthetic Multifunctional Materials Program and by the Naval Research Laboratory under a Core Research Program is gratefully acknowledged.

REFERENCES

[1] L. Christodoulou, and J.D. Venables, “Multifunctional Materials Systems: The First Generation”, *JOM*, Vol. 55, No. 12, pp. 39-45, 2003.

[2] J.D. Anderson, *Aircraft Performance and Design*, McGraw-Hill, NY, 1999.

[3] J.P. Thomas, M.A. Qidwai, P. Matic, and R.K. Everett, “Multifunctional Structure-plus-Power Concepts”, Paper # AIAA-2002-1239, 43rd AIAA/ASME/ASCE/AHS/ASC Structures, Structural Dynamics, and Materials Conference, Denver, CO, 2002.

[4] J.P. Thomas, and M.A. Qidwai, “Multifunctional Structure-Battery Materials Systems,” *JOM*, Vol. 57, No. 3, pp. 18-24, 2005.

[5] M.F. Ashby, M. F., *Materials Selection in Mechanical Design*, Butterworth-Heinemann, Oxford, 1999.

[6] J.P. Thomas, and M.A. Qidwai, "Mechanical Design and Performance of Composite Multifunctional Materials," *Acta Materialia*, Vol. 52, pp. 2155-2164, 2004.

[7] J.T. South, R.H. Carter, J.F. Snyder, C.D. Hilton, D.J. O’Brien, and E.D. Wetzel, “Multifunctional Power-Generating and Energy-Storage Composites for U.S. Army Applications”, *Proceedings of the Materials Research Society Fall Meeting: Materials for Space Applications*, Eds. M. Chipara, D. L. Edwards, S. Phillips, R. Benson, MRS Vol. 851, Boston, MA, Nov. 29 – Dec. 3, 2004.

[8] R. Kotz, and M. Carlen, “Principles and Applications of Electrochemical Capacitors”, *Electrochimica Acta*, Vo. 45, pp. 2483-2498, 2000.

[9] W.R. Pogue III, J.N. Baucom, J.P. Thomas, and M. A. Qidwai, "Structure-Power System for Unmanned Vehicles,” *CD Proceedings of AUVSI Unmanned Systems North America*, Baltimore, MD, 2005.

[10] J.P. Thomas, M.A. Qidwai, and J.C. Kellogg, “Small-Scale Energy Scavenging Concepts for Unmanned Systems”, *Journal of Power Sources*, in press.

[11] J.P. Thomas, M.T. Keennon, A. DuPasquier, M.A. Qidwai, P. Matic, “Multifunctional Structure-Battery Materials for Enhanced Performance in Small Unmanned Air Vehicles”, Paper # IMECE2003-41512, *CD Proceedings of the ASME International Mechanical Engineering Congress and Exhibition*, Washington, DC, November 15-21, 2003.

[12] M.R. Patel, *Wind and Solar Power Systems*, CRC Press LLC, Boca Raton, FL, 1999.

[13] J.L. Stone, “Photovoltaics - Unlimited Electrical Energy from the Sun,” *Physics Today*, Vol. 46, pp. 22-29, 1993.

[14] M. A. Green, K. Emery, D. L. King, S. Igari, and W. Warta, "Solar cell efficiency tables (Version 26)," *Progress in Photovoltaics: Research and Applications*, Vol. 13, pp. 387-392, 2005.

SYMPOSIA DISCUSSION – PAPER NO: 1

Author's Name: J.P. Thomas

Question (B.L. Lee):
If an inflatable structure is used for gas-spar component, how can ensure the requirement for overall structural rigidity needed to withstand aerodynamic loads?

Author's Response:
The 2 phase hydrocarbon gas (butane or propane) maintains its vapor pressure as long as any of the liquid phase remains. The vapor pressure is only a function of temperature in the 2 phase regime. The vapor pressure pushes out material of the inflatable structure, which takes the loads (i.e., it maintains the maximal section 2nd moment of aeral inertia). It also helps to prevent local buckling by maintaining an outward directed force on the material of the inflatable.
The vapor pressure can also be used to perform useful actuation work (e.g. morphing actuation), and it can also be used in a refrigeration cycle for cooling/heating.